Structure and thermal properties of the compound $Li_3AlB_2O_6$

2006 J. Phys.: Condens. Matter 18 6665

(http://iopscience.iop.org/0953-8984/18/29/008)

INSTITUTE OF PHYSICS PUBLISHING JOURNAL OF PHYSICS: CONDENSED MATTER

J. Phys.: Condens. Matter **18** (2006) 6665–6675 doi:10.1088/0953-8984/18/29/008

Structure and thermal properties of the compound $Li_3AlB_2O_6$

H Y Wu[1], H Zhang[2], X L Cheng[1,3] and Z J Liu[1]

[1] Institute of Atomic and Molecular Physics, Sichuan University, Chengdu 610065, People's Republic of China
[2] College of Physics Science and Technology, Sichuan University, Chengdu 610065, People's Republic of China

E-mail: chengxl@scu.edu.cn

Received 15 November 2005
Published 30 June 2006
Online at stacks.iop.org/JPhysCM/18/6665

Abstract

The equilibrium structure of the compound $Li_3AlB_2O_6$ is evaluated via the minimization of the total energy using pseudopotentials and a plane-wave basis within the local spin density approximation (LSDA) in the framework of density functional theory (DFT). The calculated data for the equilibrium structure are in agreement with the experimental ones. The thermal properties of $Li_3AlB_2O_6$ are consequently calculated within the quasi-harmonic approximation with the Debye model combined with the first principle for which static total energy versus volume can be calculated easily. The equilibrium volume obtained using this model also agrees with the experimental value, so other thermal outcomes gained from this model will provide overall predictions accurately for the temperature and pressure dependence of various quantities such as the equation of state (EOS), the bulk modulus, the heat capacity, and the thermal expansion.

(Some figures in this article are in colour only in the electronic version)

1. Introduction

The synthesis of optical materials has aroused great scientific interests of many scientists around the world and great progress has been made in the past several decades [1–3]. Recently, quite a number of research interests have been focused on the synthesis and characterization of inorganic borates because of the high polarizability and excellent transparency in the ultraviolet region of planar $[BO_3]^{3-}$ [4, 5] and the anisotropy of polarizability of planar $[BO_3]^{3-}$ groups. And there have been growing interests especially in lithium borates [6–8], since these

[3] Author to whom any correspondence and reprint requests should be addressed.

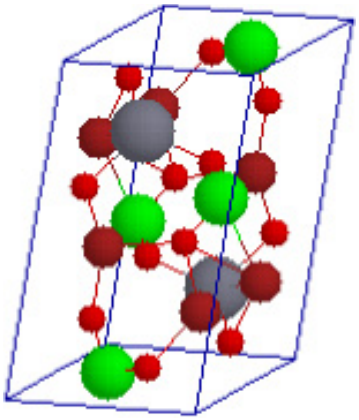

Figure 1. Crystal structure of the $Li_3AlB_2O_6$ compound proposed by Abdullaev *et al*. The largest ball is Al atom, the hypo-large ball is B atom, the smallest ball is O atom and the remainder is Li atom.

Table 1. The equilibrium lattice parameters obtained from different experiments.

	a (Å)	b (Å)	c (Å)	α (deg)	β (deg)	γ (deg)
Abdullaev *et al* [a]	6.131(2)	4.819(1)	8.227(3)	90.2(0)	117.0(0)	89.9(0)
He *et al* [b]	4.876(8)	6.191(16)	7.910(20)	74.46(18)	89.44(17)	89.52(18)

[a] Notes are referenced in [10].
[b] Notes are referenced in [11].

compounds possess a unique combination of nonlinear-optical, acousto-optical and physical properties which shows promise for a wide variety of practical applications.

$Li_3AlB_2O_6$ is a kind of ternary lithium borate compound and a new ceramic material. Its structure was first investigated by Abdullaev *et al* [9] using the x-ray powder diffraction technique as early as 1974, and then its structure was further refined in 1982 [10], as shown in figure 1. According to the reports, the compound crystallized in a triclinic unit cell with a space group of $P\bar{1}$. However, a high-resolution x-ray powder diffraction performed by He *et al* [11] confirmed the existence of $Li_3AlB_2O_6$ and exhibited that the compound also crystallized in a triclinic unit cell (space group $P\bar{1}$) as shown in figure 2. Although this structure displayed many structural similarities to the previously reported compound with the same chemical composition, its unit cell and its powder diffraction pattern were different from those reported by Abdullaev *et al* [10] as shown in table 1. Furthermore, their experimental work was difficult because Li_2O and B_2O_3 were volatile and corrosive, and in addition the temperature range of stability changed from one compound to the other. Lately, Makoto *et al* [12] prepared $Li_3AlB_2O_6$ using the conventional solid-state reaction method and found that crystallization of the compound occurred when the sintering temperature is increased from 650 to 775 °C. The x-ray powder diffraction pattern of $Li_3AlB_2O_6$ also showed a single phase which corresponded to the triclinic phase with a space group of $P\bar{1}$. Moreover, $Li_3AlB_2O_6$ ceramic was considered to be one of the attractive candidates for a LTCC (low temperature co-fired ceramic) material. Since the experimental results are mutually inconsistent and the experimental works are difficult, it is necessary to calculate the equilibrium structure of $Li_3AlB_2O_6$ theoretically. We believe that this work may be helpful in resolving the conflicts mentioned above.

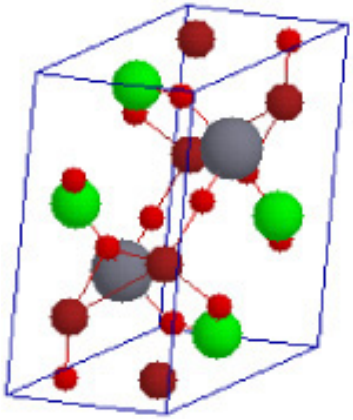

Figure 2. Crystal structure of the $Li_3AlB_2O_6$ compound proposed by He *et al*. The largest ball is Al atom, the large ball is B atom, the medium ball is Li atom, and the small ball is O atom.

In this work, we apply pseudopotentials and a plane-wave basis within the local spin density approximation (LSDA) in the framework of density functional theory (DFT) to the study of the equilibrium structure of $Li_3AlB_2O_6$ via the minimization of the total energy. We find that the calculated values for the equilibrium structure are in agreement with the experimental data. To investigate this compound in detail, the quasi-harmonic Debye model, which takes into account the thermal effects, is adopted to research the thermal properties of $Li_3AlB_2O_6$, such as the equation of state, the bulk modulus, the heat capacity, and the thermal expansion on a first principles basis. Our results demonstrate that this method can provide amply reliable predictions for the temperature and pressure dependence of these quantities.

2. Computation details

Based on the experimental data obtained from Abdullaev *et al* and those from He *et al*, the atomic positions in the unit cell are calculated using the CRYSTAL program package [13]. The plane-wave pseudopotential method and the local-density approximation (LDA) to DFT have provided a simple framework whose accuracy and predictive power have been convincingly demonstrated in a large variety of systems [14]. So our DFT calculations of the compound $Li_3AlB_2O_6$ are performed within the exchange–correlation potential in the local spin density approximation (LSDA) form suggested by Perdew and Wang [15] and a plane-wave basis set using the ABINIT code [16, 17]. Norm-conserving pseudopotentials [18] of the Troullier–Martins (TM) scheme [19] from the Fritz–Haber-Institue package for generating pseudopotentials [20] are used. With a view of accuracy of the total energy, the wavefunctions are expanded in the plane-wave basis set using a kinetic-energy cutoff radius ranging from 5 Hartree (about 136 eV) to 50 Hartree (about 1360 eV), and the k-point mesh varies from $2 \times 2 \times 2$ to $8 \times 8 \times 8$. The total energies are converged to 10^{-8} Hartree when the kinetic-energy cutoff radius is 30 Hartree (about 816 eV) and when the total energy and the ground-state wavefunctions are calculated on a $4 \times 4 \times 4$ k-point mesh over the irreducible part of the Brillouin zone.

In order to study the temperature and pressure dependence of the thermal properties, the quasi-harmonic Debye model allowing for the thermal effects is applied. By virtue of this

model, the non-equilibrium Gibbs function $G^*(V; P, T)$ is taken in the form [21]

$$G^*(V; P, T) = E(V) + PV + A_{\rm vib}(\Theta(V); T) \tag{1}$$

where the vibrational term $A_{\rm vib}$ can be written using the Debye model of the phonon density of states as [21–26]

$$A_{\rm vib}(\Theta; T) = nKT\left[\frac{9}{8}\frac{\Theta}{T} + 3\ln(1 - {\rm e}^{-\Theta/T}) - D(\Theta/T)\right] \tag{2}$$

where n is the number of atoms per formula unit, and $D(\Theta/T)$ represents the Debye integral, which is defined by [21]

$$D(y) = \frac{3}{y^3}\int_0^y \frac{x^3}{{\rm e}^x - 1}\,{\rm d}x. \tag{3}$$

In equation (1), $\Theta(V)$ is the Debye characteristic temperature of the solid. It is related to an average sound velocity, since in Debye's theory the vibrations of the solid are considered as elastic waves. It is given by [21, 22]

$$\Theta = \frac{\hbar}{k}[6\pi^2 V^{1/2} n]^{1/3} f(\sigma)\sqrt{\frac{B_{\rm S}}{M}} \tag{4}$$

where M is the molecular mass per formula unit, $B_{\rm S}$ is the adiabatic bulk modulus which measures the compressibility of the crystal for fixed quantum state populations, and $f(\sigma)$ is given in [23, 24].

Now, we can obtain the (P, T) equilibrium volume by minimizing the non-equilibrium Gibbs function $G^*(V; P, T)$ with respect to the volume V. In this way, the volumes $V_{\rm opt}(P, T)$ that minimize G^* give the thermal EOS, $V(P, T) = V_{\rm opt}(P, T)$. Because the Vinet EOS is a realistic interatomic potential function and is applicable to solids with any type of chemical bonding at present [27], further, the potential function of this EOS captures the short-range interatomic repulsion (dominant at high pressure) and short-range attraction (as in covalent and metallic solids) well. It is the overall best equation of state formulation available [28, 29], as originally noted by Vinet *et al*. We adopt the Vinet EOS fitting in our calculations [30]:

$$\ln\left[\frac{px^2}{3(1-x)}\right] = \ln B_0 + a(1-x), \qquad x = \left(\frac{V}{V_0}\right)^{1/3} \tag{5}$$

$$B_{\rm T} = -x^{-2} B_0 {\rm e}^{a(1-x)} f(x) \tag{6}$$

where $f(x) = x - 2 - ax(1 - x)$.

Finally, the isothermal bulk modulus is defined by the equilibrium thermodynamic relation

$$B_{\rm T}(P, T) = -V\left(\frac{\partial P}{\partial V}\right) = \left[V\left(\frac{\partial^2 G^*(V; P, T)}{\partial V^2}\right)_{P,T}\right]_{V_{\rm opt}(P,T)}. \tag{7}$$

After the equilibrium state for a given (P, T) has been obtained, other thermal properties can also be calculated by using the corresponding equilibrium volume in the appropriate thermal expressions. The heat capacity ($C_{v,{\rm vib}}$) is given by [21]

$$C_{v,{\rm vib}} = 3nk\left[4D(\Theta/T) - \frac{3\Theta/T}{{\rm e}^{\Theta/T} - 1}\right]. \tag{8}$$

Another property, the thermal expansion at a given temperature and pressure, is also obtained directly from the EOS; $V(P, T) = V_{\rm opt}(P, T)$ and the thermal coefficient is defined as [21]

$$\alpha = \frac{\gamma C_{v,{\rm vib}}}{B_{\rm T} V} \tag{9}$$

where γ is the Grüneisen parameter [21].

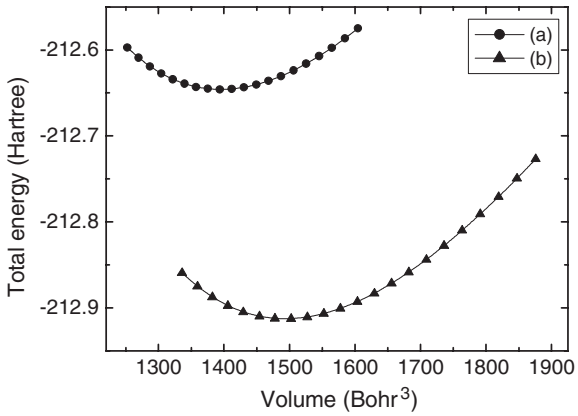

Figure 3. Static total energy as a function of volume calculated based on the experimental data from (a) Abdullaev *et al* and (b) He *et al*.

Table 2. Static equilibrium lattice parameter and volume.

	a (Å)	b (Å)	c (Å)	α (deg)	β (deg)	γ (deg)	V_0 (Å^3)
Theory	4.8136	6.1117	7.8087	74.46(0)	89.44(0)	89.52(0)	221.3138
Experiment[a]	4.876(8)	6.191(16)	7.910(20)	74.46(18)	89.44(17)	89.52(20)	230.0358

[a] Notes are referenced in [11].

3. Results and discussion

3.1. The static equilibrium lattice structure

Because this compound has very low symmetry, we have optimized the volume keeping the ratios of the axes and the angles fixed and subsequently optimized the atomic positions. The static equilibrium lattice structure is determined by minimizing the crystal total energy as a function of the volume. Figure 3 exhibits the static total energy as a function of the volume referring to the experimental data from Abdullaev *et al* (figure 3(a)) and from He *et al* (figure 3(b)). The results in figure 3 clearly indicate that the trend of variation of the total energy with volume in figure 3(a) is very similar to that in figure 3(b), and that the total energy calculated for the structure of He *et al* is lower than that calculated for the structure of Abdullaev *et al* (about 8 eV). Therefore, the structure suggested by He *et al* proves to be more stable, and we study the thermal properties of only this structure.

By fitting the E–V values from first principles to the fourth-order polynomial, the calculated volume of the structure proposed by Abdullaev *et al* is 206.7191 Å^3, which is in agreement with the corresponding experimental value 214.7577 Å^3. We obtain the resulting equilibrium volume referring to the data from He *et al*, $V_0 = 221.3138$ Å^3. The equilibrium lattice parameters and the corresponding experimental values [11] are shown in table 2, and the results are in good agreement with the experimental data (our calculated single phase which corresponds to the triclinic phase with a space group of $P\bar{1}$). At the same time, the dependence of lattice constants on volume is displayed in table 3. For further comparison, our calculated indexed powder pattern and that obtained from experiment [31] are included in table 4. It can be seen that our calculated results are also in good agreement with the experimental data obtained by He *et al* [31].

Table 3. The dependence of lattice constants on volume.

	(1)	(2)	(3)	(4)	(5)
a (Å)	4.8760	5.0114	5.0612	5.1670	5.2729
b (Å)	6.1910	6.3629	6.4262	6.5605	6.6949
c (Å)	7.9100	8.1297	8.2105	8.3821	8.5538
V_0 (Å^3)	230.0373	249.7402	257.2591	273.7377	290.9053

Table 4. List of indices and d-values from He *et al* [a] and from present work.

h	k	l	d_{obs}[a]	d_{cal} (present work)	h	k	l	d_{obs}[a]	d_{cal} (present work)
0	0	1	7.636	7.5230	1	1	2	2.9593	2.9209
0	1	0	5.970	5.8882	−1	1	2	2.9301	2.8894
0	1	1	5.465	5.3902	0	−1	2	2.8823	2.8432
1	0	0	4.881	4.8133	0	2	2	2.7314	2.6951
0	−1	1	4.1873	4.1308	0	1	3	2.6046	2.5685
1	0	1	4.1243	4.0689	0	−2	1	2.5556	2.5219
−1	0	1	4.098	4.0401	0	0	3	2.541	2.5077
0	0	2	3.8137	3.7615	1	−1	2	2.483	2.4512
1	1	0	3.7864	3.7376	−1	−1	2	2.4779	2.4448
0	1	2	3.6939	3.6434	2	0	0	2.4390	2.4066
1	1	1	3.6569	3.6101	1	2	2	2.3935	2.3627
1	−1	1	3.1775	3.1348	2	0	1	2.3281	2.2974
0	2	1	3.0717	3.0310	−2	0	1	2.3180	2.2870
−1	0	2	2.9939	2.9527	2	1	0	2.2620	2.2324

[a] Notes are referenced in [31].

3.2. The equation of state

Applying the quasi-harmonic Debye model to $Li_3AlB_2O_6$, we have obtained the equilibrium volume $V_0 = 221.2291$ Å^3, which also agrees with the experimental value [11]. For the purpose of minimizing the non-equilibrium Gibbs function $G^*(V; P, T)$ with respect to different volume V, we can fit the E–V data obtained from first principles to the Vinet equation of state.

The calculated EOS is illustrated in figure 5. The ranges of the pressure P and temperature T are from 0 to 10 GPa and from 0 to 800 K, respectively. V_0 denotes the equilibrium volume at different temperature T at $P = 0$ GPa and it varies with the temperature T as displayed in figure 4. It is noted that the ratio V/V_0 is almost linear with the pressure P at static conditions, at temperature $T = 150$ K and 750 K, respectively. At a given pressure, the ratio V/V_0 decreases as the temperature increases. As the pressure increases, the magnitude of the ratio V/V_0 decreases very quickly; at a given temperature, the ratio V/V_0 drops dramatically as the pressure increases, and there is nearly no obvious discrimination in the ratio V/V_0 at different temperatures T when the pressure $P < 1$ GPa, whereas the difference in the ratio V/V_0 is apparent gradually at different temperatures T when the pressure $P > 1$ GPa. This accounts for the fact that when $P < 1$ GPa, the effect of the temperature on the volume V nearly can be neglected; when $P > 1$ GPa, the temperature greatly influences the volume V as the pressure increases. And it can be seen that the effect of the temperature on the ratio of V/V_0 is not as important as the effect of the pressure.

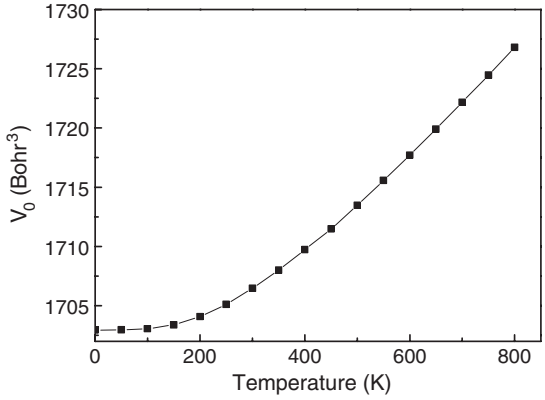

Figure 4. Variation of volume with temperature at $P = 0$ GPa.

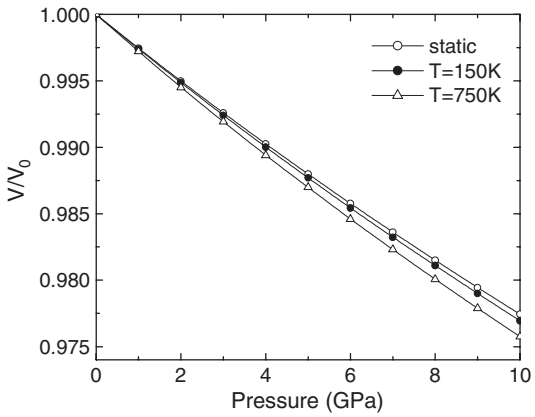

Figure 5. Calculated P–V–T relationship of $Li_3AlB_2O_6$.

3.3. Other thermodynamic properties

In figures 6 and 7, we have displayed the relations of the bulk modulus B_0 as a function of the temperature T up to 300 K at $P = 0$ GPa, and the bulk modulus B as a function of pressure P up to 10 GPa at temperatures $T = 150$ K, $T = 350$ K, $T = 550$ K and $T = 750$ K, respectively. In figure 6, we find that the bulk modulus B_0 is nearly a constant when $T < 70$ K, whereas B_0 decreases dramatically with the increment of temperature T when $T > 70$ K. This indicates that the volume varies significantly as the temperature T increases when $T > 70$ K. However, the variation of the volume is small when $T < 70$ K.

In the meantime, it is seen from figure 7 that the relationships between bulk modulus B and pressure P are nearly linear at various temperatures of $T = 150$ K, $T = 350$ K, $T = 550$ K, and $T = 750$ K, respectively. The bulk modulus B decreases with increasing temperature at a given pressure and increases with increasing pressure at a given temperature. These results are due to the fact that the effect of increasing pressure P on the material is the same as that of decreasing temperature T on the material.

Having the bulk modulus B at hand, the volume thermal expansion coefficient α can be directly derived from equation (9). The temperature and pressure dependences of the thermal expansion coefficient α are shown in figures 8 and 9. It can be seen that the thermal expansion

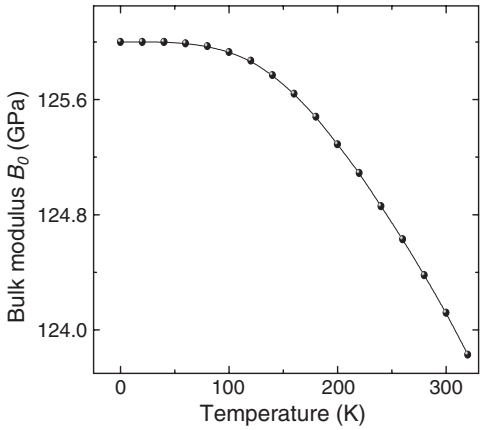

Figure 6. The bulk modulus B_0 as a function of temperature T up to 300 K at $P = 0$ GPa.

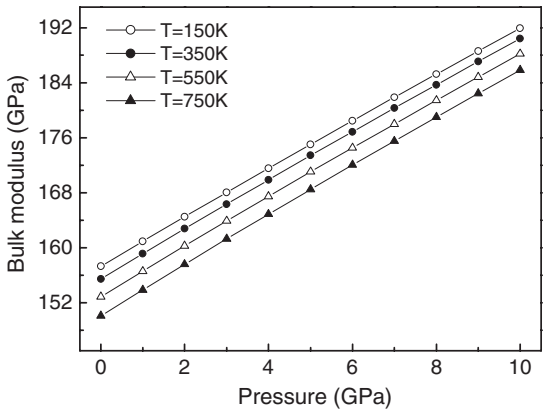

Figure 7. The relationships between bulk modulus B and pressure P at temperature of $T = 150$ K, $T = 350$ K, $T = 550$ K, and $T = 750$ K, respectively.

coefficient α increases with T^3 at low temperatures and gradually approaches a linear increase at high temperatures, and then the increasing trend becomes gentler. In figure 8, the effects of the pressure P on the thermal expansion coefficient α are very small at low temperatures; the effects are increasingly obvious as the temperature increases. However, it is noted from figure 9 that, as the pressure increases, the thermal expansion coefficient α decreases almost exponentially, and the higher the temperature is, the faster the thermal expansion coefficient α decreases. This shows that the impact of temperature is much greater than the impact of pressure on the thermal expansion coefficient α of this material. These results are in accordance with the results of the Debye theory which applies to many kinds of material.

The variation of the heat capacity at constant pressure C_P and the constant volume heat capacity C_V with temperature T and pressure P is shown in figure 10. We can notice that the variation of C_P with T is similar to that of the thermal expansion coefficient α. Nevertheless, the effect of the pressure is not as significant as that of the pressure on the thermal expansion coefficient α. At $T = 0$ K, the difference between the constant pressure heat capacity C_P and the constant volume heat capacity C_V is almost zero, but the difference increases almost linearly with the temperature T. This cannot be ignored, especially at higher temperatures,

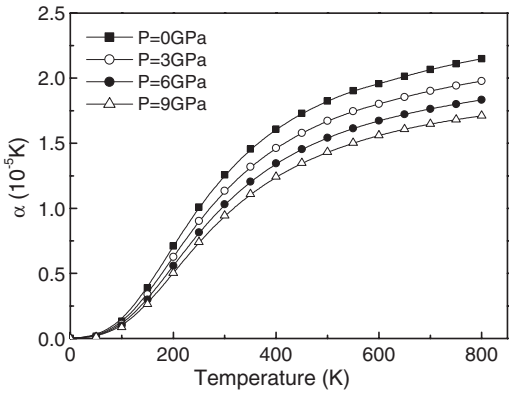

Figure 8. Variation of the thermal expansion coefficient T at pressure $P = 0$ GPa, $P = 3$ GPa, $P = 6$ GPa and $P = 9$ GPa, respectively.

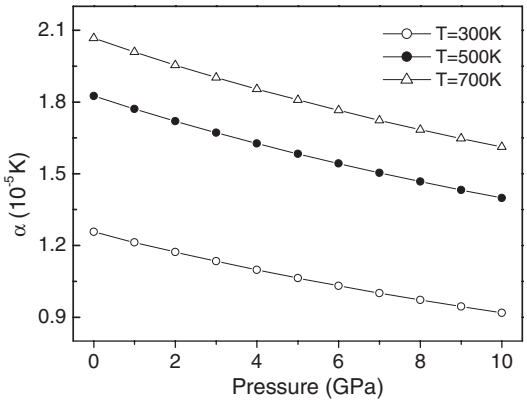

Figure 9. Variation of the thermal expansion coefficient α with pressure P at temperature $T = 300$ K, $T = 500$ K, and $T = 700$ K, respectively.

and as the temperature increases, the heat capacity at constant pressure C_P increases almost linearly with T, whereas the constant volume heat capacity C_V approaches a constant value. As the pressure increases, the difference between the constant pressure heat capacity C_P and the constant volume heat capacity C_V decreases.

4. Conclusions

In summary, the two structures suggested by He *et al* and by Abdullaev *et al* display many structural similarities, such as the same chemical composition, and both structures are described within the same space group ($P\bar{1}$), but their unit cell parameters and powder diffraction pattern were different. In this work, we have applied pseudopotentials and a plane-wave basis within DFT to the evaluation of the equilibrium structure of $Li_3AlB_2O_6$ by minimizing the total energy as the function of the volume for the two different structures. The calculated results are in agreement with their corresponding experimental values. We find that the structure suggested by He *et al* proves to be more stable owing to its total energy being lower than that of the structure proposed by Abdullaev *et al*. Then the quasi-harmonic Debye model which combines

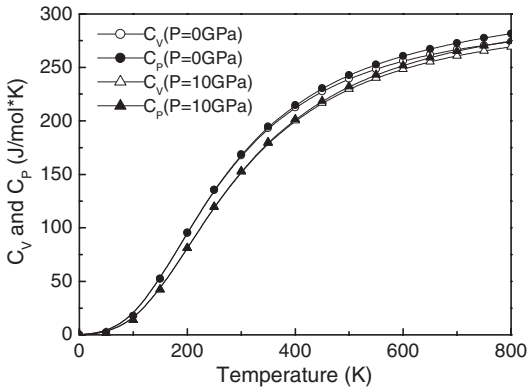

Figure 10. Variation of the heat capacity C_P and C_V with temperature under different pressures.

with the *ab initio* calculation of the static total energy was adopted to calculate the temperature and pressure dependence of the thermal properties. The calculated equilibrium volume using this model also agrees with the corresponding experimental data. Therefore, the results of other thermal characteristics obtained from this model will also offer reliable predictions for the temperature and pressure dependence of these various quantities, such as the equation of state, the bulk modulus, the heat capacity, and the thermal expansion. Furthermore, it is found that although $Li_3AlB_2O_6$ is a sort of complex polyatomic ternary compound, the trend of variation of some of its thermal properties with temperature and pressure is similar to that of a number of simple crystals. Our research work on the properties of this compound will be helpful for understanding this compound more.

Acknowledgments

We thank X Gonze *et al* for providing us their ABINIT code. This work is financially supported by the National Natural Science Foundation of China and China Academy of Engineering Physics under grant No. 10376021 (NSAF).

References

[1] Katz L and Megaw H D 1967 *Acta Crystallogr.* **22** 639
[2] Abrahams S C and Marsh P 1986 *Acta. Crystallogr.* B **42** 61
[3] Chen C, Wu B, Jiang A and You G 1985 *Sci. Sin.* B **28** 235
[4] Becker P 1998 *Adv. Mater.* **10** 979
[5] Keszler D A 1999 *Curr. Opin. Solid State Mater. Sci.* **4** 155
[6] Jiang A D, Lei S R, Huang Q Z, Chen T B and Ke D M 1990 *Acta Crystallogr.* C **46** 1999
[7] KmFEL A and WmL G 1983 *Acta Crystallogr.* B **39** 175
[8] Chen C, Wu Y, Jiang A, Wu B, You G, Li R and Lin S 1989 *J. Opt. Soc. Am.* B **6** 616
[9] Abdullaev G and Mamedov K 1974 *Kristallagrafiya* **19** 165
[10] Abdullaev G and Mamedov K 1982 *Kristallagrafiya* **27** 381
[11] He M, Chen X L, Hu B Q, Zhou T, Xu Y P and Xu T 2002 *J. Solid State Chem.* **165** 187
[12] Makoto O, Hirotaka O, Akinori K and Eri T 2005 *J. Eur. Ceram. Soc.* **25** 2877
[13] Saunders V R, Dovesi R, Roetti C, Caus'a M, Harrison N M, Orlando R and Zicovich-Wilson C M 1998 *CRYSTAL98 User's Manual* Torino
[14] Giannozzi P, de Gironcoli S, Pavone P and Baroni S 1991 *Phys. Rev.* B **43** 7231
[15] Perdew J P and Wang Y 1992 *Phys. Rev.* B **45** 13244

[16] Gonze X, Beuken J-M, Caracas R, Detraux F, Fuchs M, Rignanese G-M, Sindic L, Verstraete M, Zerah G, Jollet F, Torrent M, Roy A, Mikami M, Ghosez Ph, Raty J-Y and Allan D C 2002 *Comput. Mater. Sci.* **25** 478
[17] The ABINIT code is a common project of the Universite Catholique de Louvain, Corning Incorporated, and other contributors (URL http://www.abinit.org)
[18] Topp W C and Hopfield J J 1973 *Phys. Rev.* B **7** 1295
[19] Troullier N and Martins J L 1991 *Phys. Rev.* B **43** 1993
[20] Fuchs M and Scheffler M 1999 *Comput. Phys. Commun.* **119** 67
[21] Blanco M A, Francisco E and Luaña V 2004 *Comput. Phys. Commun.* **158** 57
[22] Blanco M A 1997 *PhD Thesis* Universidad de Oviedo (URL http://web.uniovi.es/qcg/mab/tesis.html)
[23] Blanco M A, Martín Pendás A, Francisco E, Recio J M and Franco R 1996 *J. Mol. Struct. Theochem.* **368** 245
[24] Francisco E, Recio J M, Blanco M A and Martín Pendás A 1998 *J. Phys. Chem.* **102** 1595
[25] Francisco E, Sanjurjo G and Blanco M A 2001 *Phys. Rev.* B **63** 094107
[26] Flórez M, Recio J M, Francisco E, Blanco M A and Martín Pendás A 2002 *Phys. Rev.* B **66** 144112
[27] Holzapfel W B 2001 *Z. Kristallogr.* **216** 473
[28] Hama J and Suito K 1996 *J. Phys.: Condens. Matter* **8** 67
[29] Cohn R E, Gulseren O and Hemley R J 2000 *Am. Mineral.* **85** 338
[30] Vinet P, Rose J H, Ferrante J and Smith J R 1989 *J. Phys.: Condens. Matter* **1** 1941
[31] He M, Chen X L, Gramlich V, Baerlocher Ch, Zhou T and Hu B Q 2002 *J. Solid State Chem.* **163** 369